N.Fusun OYMAN SERTELLER[1], Yasin BEKTAS[2], Selçuk NOGAY[3], Tahir Cetin AKINCI[3]

Marmara University (1), Marmara University (2), Kirklareli University (3)

Speed Estimation of Brushless Direct Current (BLDC) Motor with Multilayer Perceptron

Abstract. *This study used an artificial neural network model to estimate the revolutions per minute of a brushless direct current (BLDC) motor operating at different driver modes and different load currents. The dataset that was used to train and test the artificial neural network model was obtained from experimental applications and was made applicable for the training of a multilayer perceptron. A total of 7643 data items were used in the study. Of these data, 382 were used to test the ANN model. Test results indicated that the multilayer perceptron provided 99.34% estimation and that the target and the results were quite close.*

Streszczenie. *W artykule zaprezentowano wykorzystanie sieci neuronowej do określania prędkości obrotowej bezszczotkowgo silnika BLDC pracującego przy różnych prądach obciążenia. Do trenowania sieci użyto danych eksperymentalnych. (**Określanie prędkości obrotowej silnika BLDC przy wykorzystaniu wielowarstwowego perceptronu**)*

Keywords: Multi–layer perceptron, Bacpropagation, Brushless Direct Current Motor (BLDC), Speed, Estimation.
Słowa kluczowe: sieci neuronowe, silnik BLDC

Introduction

Brushless Direct Current (BLDC) motors are used in a wide variety of fields due to their high efficiency, high startup moment and silent operation. To operate brushless DC motors, a control system and sensors that determine rotor position are required. Systems that can be controlled without sensors were developed due to advances in technology.

A brushless direct current (BLDC) motor provides commutation operation electronically instead of mechanically. In brushed DC motors, electric conduction to the windings in the rotor is provided via a brush-collector structure. Due to the sectional structure of the collector mechanism, the direction of the current passing through the rotor windings automatically changes while the motor turns. This system creates some problems, including formation of sparks, servicing requirements and wear in brushes [1].

In brushless direct current motors, the function of the brush-collector mechanism is undertaken by a controller. The controller includes semi-conductive circuit components that serve to switch high current and a micro controller, which adjusts the timing of the switching. To avoid any disruption in the rotation of the motor, the controller should follow the rotor at an appropriate speed. For this operation, the rotor position should be known. In many applications, rotor position is easily identified using Hall effective sensors [2,3].

As in all control systems, any method used to control a brushless direct current motor is based on the identification of motor position and speed. In this study, the motor speed (rpm) of a brushless direct current motor fed by a unipolar-bipolar driver was determined using an artificial neural network model at different operation modes of the driver (unipolar, bipolar, unipolar), different motor loads and load currents. The study used a multilayer perceptron estimation model. The data set used to train the model was obtained from 15 experimental applications performed with the brushless direct current motor. The model was trained using a back-propagation learning algorithm and the system was tested using a total of 382 test data. Test results indicated that there was a close relationship between the output of the ANN model and the target.

Structure of this paper is as follows:

In Section 2, general information about the functioning of ANN is given. Levenberg-Marquardt back propagation learning algorithm has been mentioned briefly.

In Section 3, installation of the experimental set up and obtaining the data set is described.

In Section 4, normalization of the data set, architecture of ANN model and training process of the model are described.

In Section 5, testing the model and tests results is presented.

In Section 6, results and discussions of the study are presented.

In Section 7, conclusions of the study is presented.

Artificial Neural Network (ANN)

ANNs are mathematical systems consisting of many weighted interconnected operation elements (neurons). A processing element is an equation, which is often termed a transfer function. This processing element receives signals from other neurons; combines and converts them; and produces a numerical result. In general, processing elements roughly correspond to real neurons, they are interconnected via a network and this structure constitutes neural networks [4].

The structure of ANNs contains three main elements: neurons, the connection providing input and output route, and connection weights indicating the strength of these connections. Typically, the architecture (structure) of an ANN is formed and weight values required to optimize the accuracy of the outputs are determined using one of several mathematical algorithms. The ANNs unravel a relationship between the input variables and estimated variables by determining the weights using previous examples. In other words, ANNs are "trained".. Once these relationships are determined (in other words, once the network is trained), an ANN can be operated with new data and estimations can be produced. The performance of a network is measured by the aimed signal and error criterion. The error margin is obtained by the comparison of the output of the network and the aimed output. A back-propagation algorithm is used to adjust the weights in such a way to reduce the error margin. The network is trained by repeating this processing many times. The aim of training is to reach an optimum solution based on performance measurements [4-6].

ANNs have an extensive range of applications in real-life problems. They are currently used successfully in many industries. There is no restriction in the fields of application; however they are more heavily used in fields such as estimation, modeling and classification. Although ANNs first appeared in the 1950s, they reached sufficient level for general use in the mid-1980s. Today, ANNs are utilized in an increasing range of complex problems. As an artificial neural network is the model which best defines trends or patterns in the data, they are very appropriate for prediction and prediction processes [6].

Today there are many ANN models that are applied to different problems. The most common models in the multilayer perceptron models, trained with a back-propagation learning algorithm. The model used in the present study, a multilayer perceptron trained with a back-propagation learning algorithm, is presented in Figure 1. As can be seen from Figure 1, the model used in the study has 20 neurons in the hidden layer. A total of 5 neurons were used in the input layer and 1 neuron was used in the output layer [4-6].

The "Levenberg-Marquardt learning algorithm" was used as the back-propagation learning algorithm to train the ANN model.

The back-propagation learning algorithm is presented below in brief. For each neuron in the input layer, the neuron outputs are given by

$$n_i = o_i \tag{1}$$

where ni is the input of neuron i, and oi the output of neuron i. Again for each neuron in the output layer, the neuron inputs are given by

$$n_k = \sum_{j=1}^{N_j} w_{kj} o_j \tag{2}$$

where wkj, is the connection weight between neuron j and neuron k, and Nj, Nk the number of neurons in the hidden layer and output layer, respectively. The neuron outputs are given by

$$o_k = \frac{1}{1+\exp[-(n_k+\theta_k)]} = f_k(n_k, \theta_k) \tag{3}$$

where θk is the threshold of neuron k, and the activation function fk is a sigmoidal function. For the neurons in the hidden layer, the inputs and the outputs are given by relationships similar to those given in Eqs. (2) and (3), respectively.

The connection weights of the feed-forward network are derived from the input–output patterns in the training set by the application of generalized delta rule. The algorithm is based on minimization of the error function on each pattern p by the use of steepest descent method. The sum of squared errors Ep which is the error function for each pattern is given by

$$E_P = \frac{1}{2}\sum_{k=1}^{N_k} \left(t_{pk} - o_{pk}\right)^2 \tag{4}$$

where tpk is the target output for output neuron k, and opk the calculated output for output neuron k. The overall measure of the error for all the input–output patterns is given by

$$E = \sum_{p=1}^{N_p} E_p \tag{5}$$

where Np is the number of input–output patterns in the training set. When an input pattern p with the target output vector tp is presented, the connection weights are updated by using the following equations:

$$\Delta w_{kj} = \eta \delta_{pk} o_{pj} + \alpha \Delta w_{kj}(p-1) \tag{6}$$

$$\delta_{pk} = \left(t_{pk} - o_{pk}\right) o_{pk}\left(1 - o_{pk}\right) \tag{7}$$

where η is the learning rate, and α is the momentum constant. Again, the connection weights between input layer neuron i and hidden layer neuron j can be updated by using the following equations:

$$\Delta w_{ji} = \eta \delta_{pk} o_{pj} + \alpha \Delta w_{ji}(p-1) \tag{8}$$

$$\delta_{pj} = o_{pj}\left(1 - o_{pj}\right)\sum_{k=1}^{N_k} \delta_{pk} w_{kj} \tag{9}$$

It is important to note that the threshold θ of each neuron is learned in the way same as that for the other weights. The threshold of a neuron is regarded as a modifiable connection weight between that neuron and a fictitious neuron in the previous layer which always has an output value of unity [7-10].

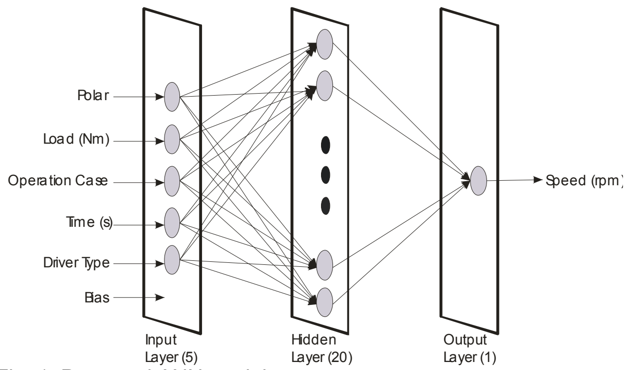

Fig. 1. Proposed ANN model

In order to use the ANN simulator for any application, first the number of neurons in the layers, type of activation function (purelin, tansig, logsig), the number of patterns, and the training rate must be chosen.

Experimental Applications and Data Set Creation
Experimental set of the driving circuit of the BLDC motor

The realized education tool of the BLDC motor is shown schematically in fig. 2. The real set is shown in fig.3 (a) and (b) [11-13].

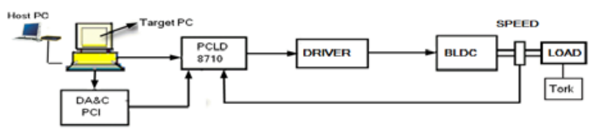

Fig.2. Schematic diagram of the BLDC motor, its driving circuit and its other auxiliaries

The experiment set of BLDC motor including the loading equipment as an educational tool is presented in fig.2. The developed flow diagram is given in Appendix II. Figure 3 (a) show complete part of the experiment set and figure 3 (b) shows the main components of the experiment set.

One of the most powerful aspects of MATLAB functions is to present useful functions package which are called toolbox. Toolbox covers wide range of application areas such as mathematics, analysis, modeling, data collection, control, signal and image processing and cost modeling so on. These are additional functions and enable us to run in real time on our laptop PC for rapid prototyping or hardware-in-the-loop simulation of control system.

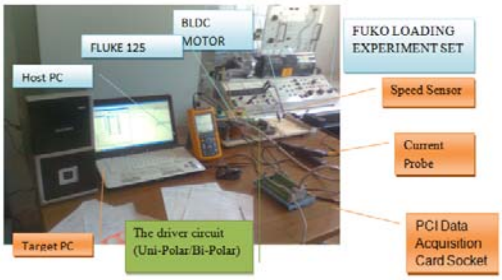

(a)

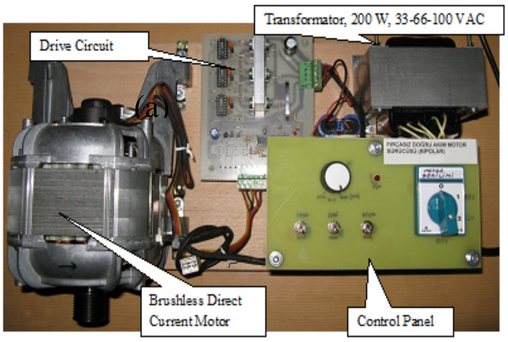

(b)

Fig.3. (a). The whole experimental set which includes loading equipment and other auxiliaries (a), BLDC motor with its driving unit (b).

Since control technology of BLDC motor is predominantly explained in this study, special interest is given to driving circuit. It can be explained in three sections in general. In the first section, a controller that processes the position information coming from the sensors is available with electronic component (MC33035).

The position information processed by the controller is used to trigger the six switching element (IRF720) for the bipolar working mode and three switching (in some cases this number can be increased) that can be named as second section.

The third section in the circuit consists to ensure the insulation of MOSFET drive circuit elements (IR2113) between the section that belongs to the keying elements where the high source voltage is available and the section that belongs to the controller where low voltage is available and hall sensors to define rotor position(SA, SB, SC) [13-19].

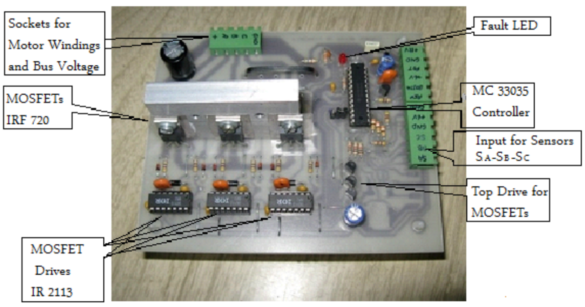

Fig.4. Driving card of the BLDC motor with its all equipments.

Terminal voltage is distributed to the motor over the switching elements (MOSFETs) determined and triggered by the controller according to the position of the rotor (see Figure 4).

Bipolar and unipolar circuit driving system

Three- phase stator windings (A,B,C) star -connected BLDC motors (see in Figures 5 and 6) can be categorized as bipolar or unipolar driving systems like identical other type of motors.

Unipolar and bipolar driving methods energize one phase and two phases out of three phases at each commutation period, respectively. Their commutation periods are 60 and 120 electrical degrees, respectively.

The unipolar driving system has fewer electromagnetic switches (see in Figure 1) and a simpler driving circuit and the commutation frequency is half that of the bipolar driving circuit.

A unipolar drive appears to offer advantageous over the bipolar drive. However, during start-up operation, magnetic saturation appears due to huge current values, and this causes high torque ripple and lower starting torque. Additionally, it has dead spots like a single phase motor, because the direction of current flows through the phase windings can not be inverted [20,21].

The current flow direction and current values are given Figures 6(a) and 7(b).

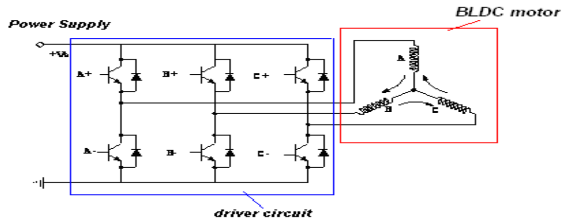

(a)

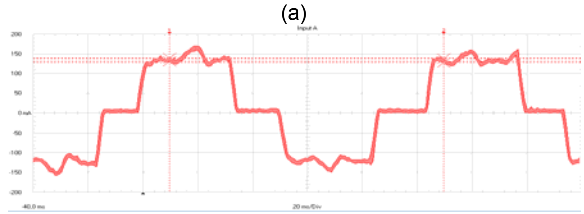

(b)

Fig.5. Bipolar driver circuit and stator windings of motor (a) stator current values for phase A

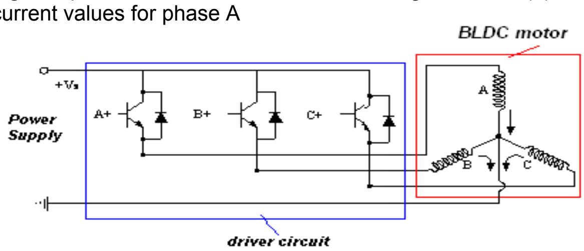

(a)

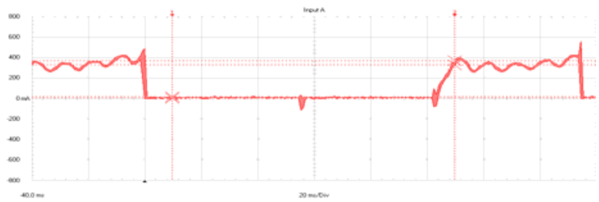

(b)

Fig. 6. Unipolar driver circuit and stator windings of motor (a) stator current valuesfor phase A(b)

Hybrid (Bipolar- starting and unipolar-running) driving system

The bipolar-starting and unipolar-running method is used to provide high speed with high starting torque, especially when the motor is loaded. As a result, a bipolar starting and unipolar-running driving circuit is thought to combine advantages of bipolar and unipolar driving.

In Figure 7 shows another topology of a unipolar drive with six switches (transistors). Since the unipolar drive use three switches and they can't invert the direction of the current flow with the application of two additional switches current flow can be inverted. These two switches (N+ and N-) are connected to a neutral point and they are off using bipolar drive (stating time). In the case of operating unipolar drive two additional switches play role on flowing the positive or negative current in the given single phase.

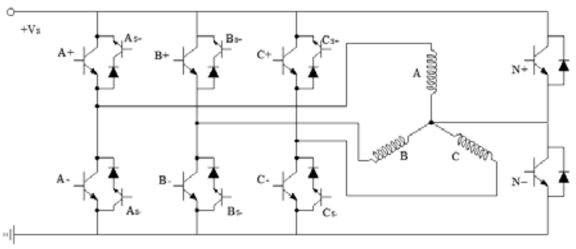

(a)

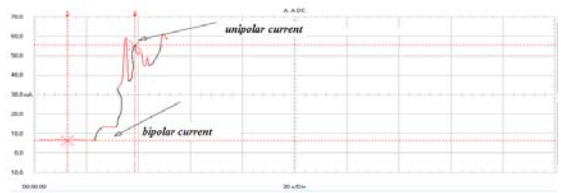

(b)

Fig.7. Hybrid driver circuit and stator windings of BLDC motor(a) bipolar starting unipolar running driver current variation.

Data set creation

A total of 15 tests were performed to obtain the data set that was used to train and test the artificial neural network. Each test was performed at different load currents of the BLDC motor with different driver types and at different levels of the driver (unipolar, bipolar), and numerical and graphical data was obtained. As indicated in Table 1, the speed-time graph obtained from each individual test was enumerated for different operation modes of the motor to be used in the data set. In addition, since the driver level and driver type will be used in the data set, they were enumerated as indicated in Table 1. This enumeration was performed randomly, according to the preference of the designer.

Table 1 Numbering

Stage	Bipolar	1
	Unipolar	2
Operation Case	Initial	3
	Tansient1	4
	Optimum	5
	Transient2	6
	Finish	7
Driver Type	Uni-Bipo	8
	Bipolar	9
	Unipolar	10

As indicated in Table 2, the speed-time graph or speed-data number obtained from each of the 15 experimental applications were named for different operation modes. The intervals between data points used in the data set are presented in Table 2.

Table 2. Operation Cases

No	Data Points of Operation Cases				
	Initial	*Transient 1*	*Optimum*	*Transient 2*	*Finish*
1	013-024	175-195	305-335	565-585	862-882
2	002-050	166-311	323-566	567-843	844-950
3	002-030	219-336	370-436	594-725	726-799
4	002-040	183-311	312-370	536-663	664-776
5	002-030	165-273	274-326	513-628	684-760
6	002-050	058-293	294-380	424-942	943-961
7	002-040	142-256	397-445	541-703	744-800
8	002-040	141-273	274-341	532-659	660-740
9	002-040	102-189	210-340	380-511	512-576
10	002-033	125-218	300-400	561-673	674-906
11	002-030	113-237	240-340	344-779	780-906
12	002-040	179-302	332-460	525-671	672-750
13	002-040	193-321	322-422	555-687	688-780
14	002-030	050-158	170-220	350-495	496-597
15	002-030	100-214	215-269	415-538	540-570

Fig. 8. indicates the speed-data route graph for the first of 15 tests. The red line shows the intervals corresponding to operation mode with explanations.

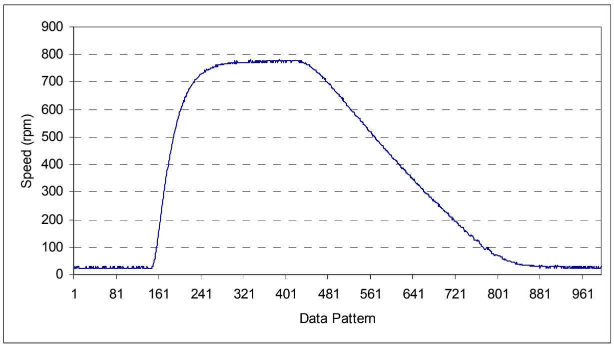

Fig. 8. Overall speed variation of the BLDC motor for experiment 1

Since the study included a total of 15 speed graphs like the one in Figure 8, only one was presented as an example. A total of 7643 data items were used to train and test the model. Of these data, 382 were used to test the ANN model and 382 were used to confirm the model. Table 3 presents a summary showing only maximum and minimum values of the data set [22].

Table 3. Summary of Data Set

		Max.	Min.
Output	Speed (rpm)	1450.195	19.5312
Inputs	Polar	2	1
	Load (Nm)	0.5	0
	Operation Case	7	3
	Time (s)	9.6	0.01
	Driver Type	9	8

Designing and Training Process of the ANN Model

An artificial neural network model is designed in five steps: data collection, normalization of data, and selection of architecture of the ANN model, training of the network and testing of the network. Normalization of data is a process of scaling the numbers in a data set to improve the accuracy of the subsequent numeric computations and is an important stage in training the ANN. Normalization also helps in shaping the activation function. For this reason, a [+1, -1] normalization function was used. To select the architecture of the artificial neural network, it is very important to determine the number of layers and number of neurons in each layer. There are no fixed criteria for this initiative, and these parameters are selected only by the designer of the ANN model, according to his/her initiative. The general application is to select the most commonly preferred parameters according to the type of problem.

There are only general rules picked up over time and followed by most researchers and engineers applying this architecture to their problems. The first rule states that if the complexity in the relationship between the input data and the desired output increases, then the number of the processing elements in the hidden layer should also increase. The second rule says that if the process being modeled is separable into multiple stages, then additional hidden layer(s) may be required. The result of the tests has showed that the optimal number of neurons in the hidden layer can be chosen as 20 also, the activation function has been chosen as a hyperbolic tangent sigmoid function for all of the layers [22].

In this study ANN was trained with the back propagation (Levenberg – Marquardt) training algorithm. In the training process of this study, the actual output of ANN was compared with the desired output. The training set consists of sixteen nput and five output data to the ANN model. The number of data was 7643. 90% of this data were used for training. The network adjusted the weighting coefficients that began with random set. The training process has been stopped when the error has become stable. ANN simulator has been trained through the 128 epochs as shown in Figure 9.

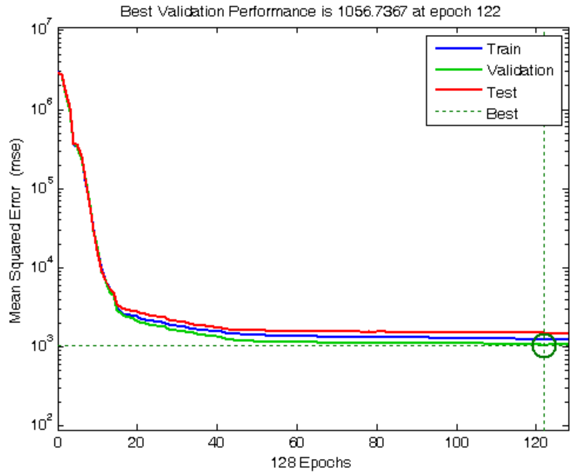

Fig.9. Performance of the system

Testing the ANN Model

In the test, an unknown input pattern has been presented to the ANN, and the output has been calculated. Linear regression between the ANN output and target is performed. After ANN learning, test and validation steps founded regression coefficients (R = 0.994148, R = 0.993468 and R =0.994874) shows that target and ANN output values were very related each other. These regression analyses were shown in Figure 10 for learning, validation and testing steps [22]. Also in Table 4, performance of the ANN system is illustrated.

Results and Discussions

A total of 5 inputs and 1 output were used in the created ANN model. The model was designed in three layers. The first layer is an input layer; the second layer is a hidden layer and the third layer is an output layer. The number of neurons (processing element) used in the hidden layer was 20. According to the results shown Table 4, the model was trained at a level of 99.34%.

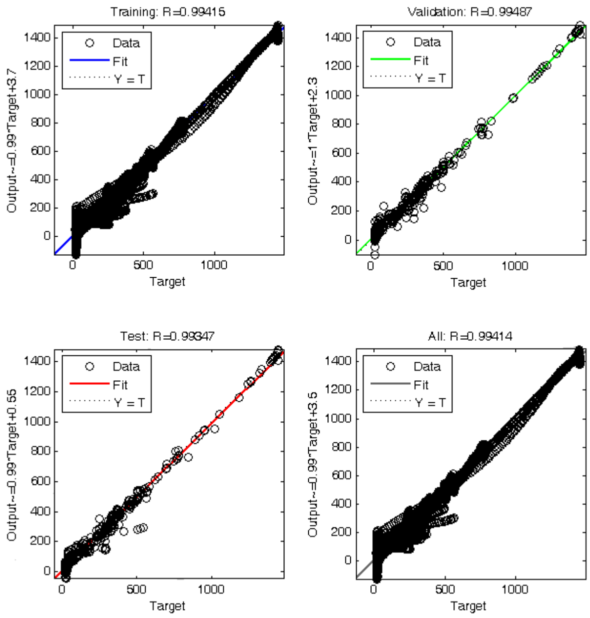

Fig.10. Regression graphs of the ANN system

Table 4. Results of ANN model

	Samples	MSE	RMSE	R
Training	6879	1232.4311	35.105998	0.994148
Validation	382	1056.7367	32.507486	0.994874
Testing	382	1496.9407	38.690317	0.993468

The system was tested with the test data and an estimation of 99.34% was achieved. It is understood from the performance curve that mean square error (MSE) values decreased by one thousand fold, from six digit values to three digit values at the end of the 128th iteration. The graph in Figure 11 shows that the real values and target values are quite similar

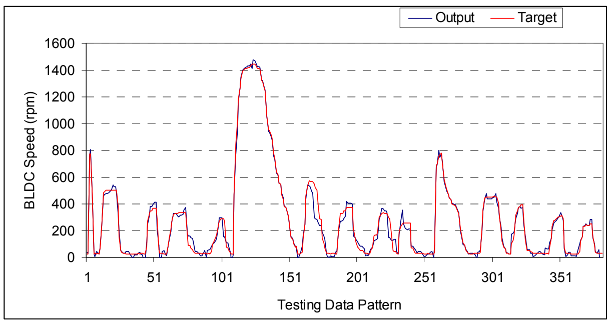

Fig.11. Comparison of the ANN results and Targets

Conclusion

In this study, an ANN model was developed to estimate rotor speed (revolutions per minute (rpm)) of a brushless direct current (BLDC) motor for different operation modes at different loads. A multilayer perceptron approach was used in the study. Experimental applications were conducted to obtain the data set that was used in the ANN model. As a result of these experiments, speed curves at different load currents and different driver levels at 0.01 second sampling rates were obtained. These speed curves were enumerated for different operation areas and formed the data set used to rain the ANN.

In this study:

- Speed and current moment curves were obtained by performing a total of 15 tests using a brushless direct current motor.
- Speed-time analyses were performed based on the obtained data.
- A data set was created based on the speed-data graphs.
- A multilayer ANN model was developed; this ANN model was trained by a back-propagation learning algorithm using 90% of the created data set, and system success was tested using 10% of the data set.
- The revolutions per minute of the brushless direct current motor were estimated at different operation points, different loads and different operation conditions with a ratio of 99.34%.
-

The study indicated that the experimental results obtained from brushless direct current motor and ANN outputs were significantly consistent.

REFERENCES

[1] Juan W. Dixon, Ivan Leal; Current control strategy for brushless dc motors based on a common dc signal. *IEEE Transactions on Power Electronics*, 17(2), March (2002).

[2] K.S. Low M.F. Rahman and K.W. Lim. Approaches to the control of torque and current in a brushless dc drive. March-April (2005).

[3] Texas Instruments Incorporated. DSP Solutions for BLDC Motors, (1997).

[4] Yurtoglu H.,Yapay Sinir Ağları Metodolojisi ile Öngörü Modellemesi: Bazı Makroekonomik Degişkenler İçin Türkiye Örneği. February, T.C. DPT, (2005).

[5] Alexander, I. ve Morton, H.; An Introduction to Neural Computing, London: Chapman and Hall, 1990.

[6] Anderson, D. ve McNeil, G.; Artificial Neural Networks Technology, Data & Analysis Center for Software, *Kaman Sciences Corparation*, (1992), Newyork, USA.

[7] Aydogmus Z., A neural network-based estimation of electric fields along high voltage insulators. Expert Systems with Applications (2009), 36,8705–8710.

[8] Hagan T.M., Demuth HB, Beale M., Neural Network Design. *PWS Publishing Company*, Boston, 1996,pp.2-44.

[9] Bose B.K.; Modern Power Electronics and Ac Drives, *Prentice Hall PTR*, USA, (2002), 625-689.

[10] Nogay, H.S., Prediction of Internal Temperature in Stator Winding of Three-Phase Induction Motors with ANN, *European Transactions on Electrical Power*, 20:1–9. DOI: 10.1002. 2010.

[11] Akcayol, M.A., Cetin A, Elmas, C,; An educational tool for fuzzy logic-controlled BDCM, (2002), 45, 33-42.

[12] Gotou, M., Ochi, M., A new drive system of a brushless motor reducing power consumption and motor vibration simultaneously, *IEEE International Conference on power electronics and drive systems*, PEDS'99, July (1999), Hong Kong.

[13] Sway C.L.P., Singh, B., Singh, B.P., Murty, S.S.; Experimental investigations on a Permanent Magnet Brushless DC motor fed by a PV array for a water pumping system, *Journal of solar energy*, (2000), 122, 129-130.

[14] Karady, G.G., Increasing student interest and comprension in power engineering education at the graduate and undergraduate level, (2000), 1, 12-21.

[15] Park, S.J., Park H.W., Lee M.H.; Harashima, F, A new approach for minimum torque ripple maximum efficiency control of BLDC, (2000), 47, 109-114.

[16] Bolton HR, Ashen RA, Influence of motor design and feed-current wave form on torque ripple in brushless DC drive Proc. Ins. Elec. Eng. 1984,131, pp.82-90.

[17] Haskew, T.A, Schinstock D.E, Bredeson J.G., Salem E.T.; Brushless machine monitoring and simulation Proceedings of the Intersociety, *Energy Conversion Engineering Conference*,Washington DC USA, Agust 11-16, (1996).

[18] Haskew, T.A., Jackson, D.J.; Real-time simulation methods for a six-pulse converter *Electric Power Systems Research,* (1995),33, 69-75.

[19] Bodner, G.M., Why good teaching fails and hard working students do not always succeed. Spec (1990), 28, 27-32.

[20] Jang, G, Kim, MG,; A bipolar starting and unipolar running method to drive a hard disk drive spindle motor at high speed with large starting torque 2005,41, pp.750-755.

[21] Zhong, M.P., Zheng, S.Y. Pan, X.H.;Design of direct-drive air compressor drived by permanent magnet brushless DC motor Engineering Science, (2009), 43, 495-499.

[22] Akinci, T.C., Nogay, H.S.,Gokmen,G., Determination of Optimum Operation Cases in Electric Arc Welding Machine, Using Neural Network, *Journal of Mechanical Science and Technology*, (2011),25 (4), 1253-1260.

Authors: *Assoc Prof. Dr. N.Fusun Oyman Serteller, Marmara University, Faculty of Technology, Department of Electrical & Electronics Engineering, Istanbul-Turkey.*
E-mail: fserteller@marmara.edu.tr.
Ms.C. Yasin Bektas, Marmara University, Technical Education Faculty, Istanbul-Turkey.
E-mail: yasinbektas@yahoo.com.
Assoc Prof.Dr. H.Selcuk Nogay, Kirklareli University, Engineering Faculty Department of Electrical & Electronics Engineering Kirklareli-Turkey.
E-mail:hidirselcuknogay@gmail.com.
Assist Prof.Dr. Tahir Cetin Akinci, Kirklareli University, Engineering Faculty Department of Electrical & Electronics Engineering Kirklareli-Turkey.
E-mail: cetinakinci@hotmail.com.